Electronic Supplementary Material (ESI) for Journal of Materials Chemistry A.

Electronic Supplementary Information

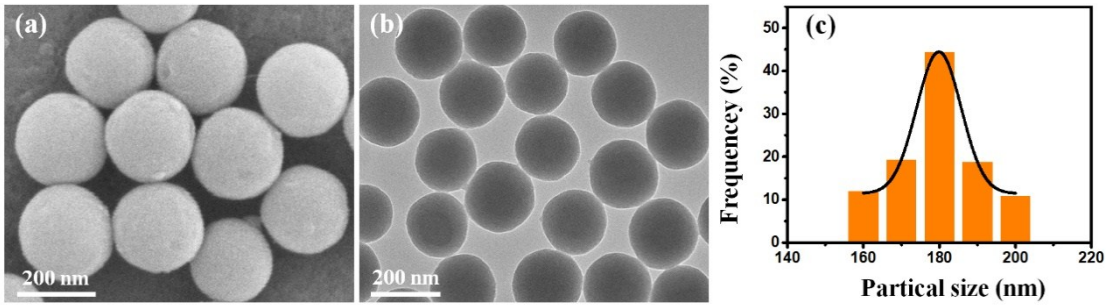

Fig. S1 (a) SEM image, (b) TEM image and (c) particle-size distribution histogram of the SiO_2 spheres.

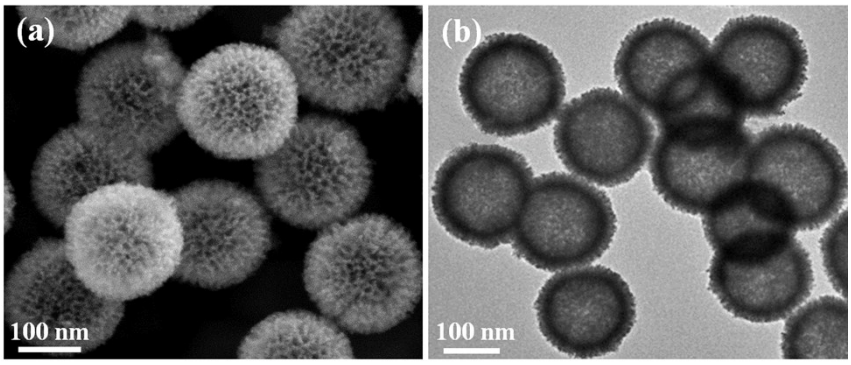

Fig. S2 (a) SEM and (b) TEM images of the Pt MNCs.

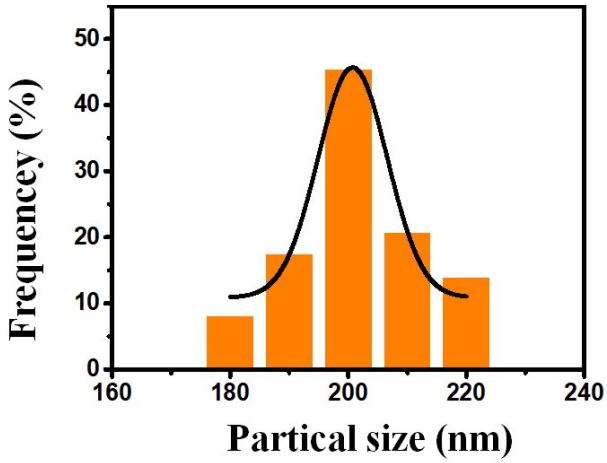

Fig. S3 Particle-size distribution histogram of the Pt-Ni-P MNCs.

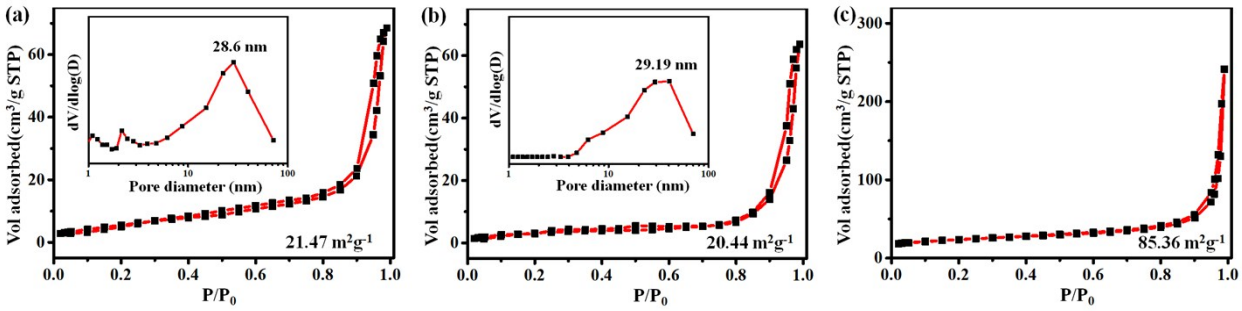

Fig. S4 N_2 adsorption-desorption isotherms for (a) Pt-Ni-P MNCs , (b)Pt-Ni MNCs , and (c) Pt/C. The insets in (a) and (b) are the BJH pore-size distribution curves.

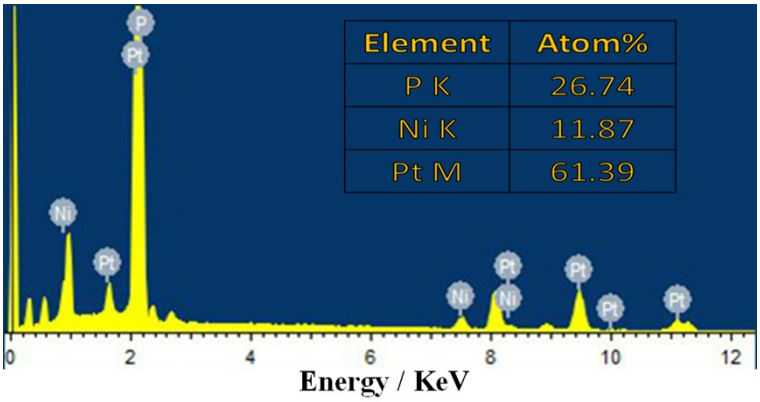

Fig. S5 EDX spectrum of the Pt-Ni-P MNCs.

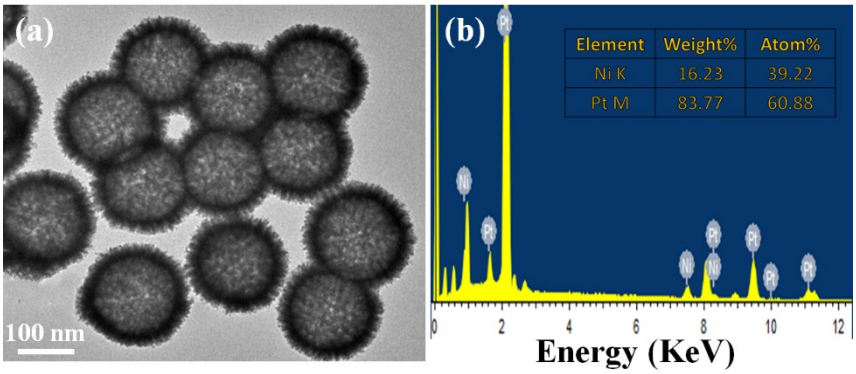

Fig. S6 (a) TEM image and (b) EDX spectrum of the Pt-Ni MNCs.

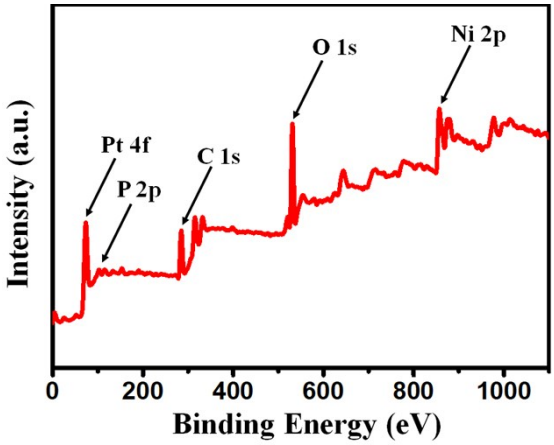

Fig. S7 XPS survey spectrum for the Pt-Ni-P MNCs.

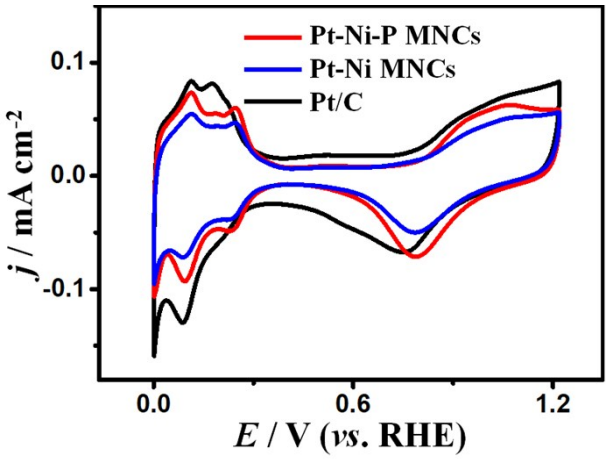

Fig. S8 Cyclic voltammogram curves of the electrocatalysts recorded in a N_2-saturated 0.5 M H_2SO_4 solution at a scan rate of 50 mV s^{-1}.

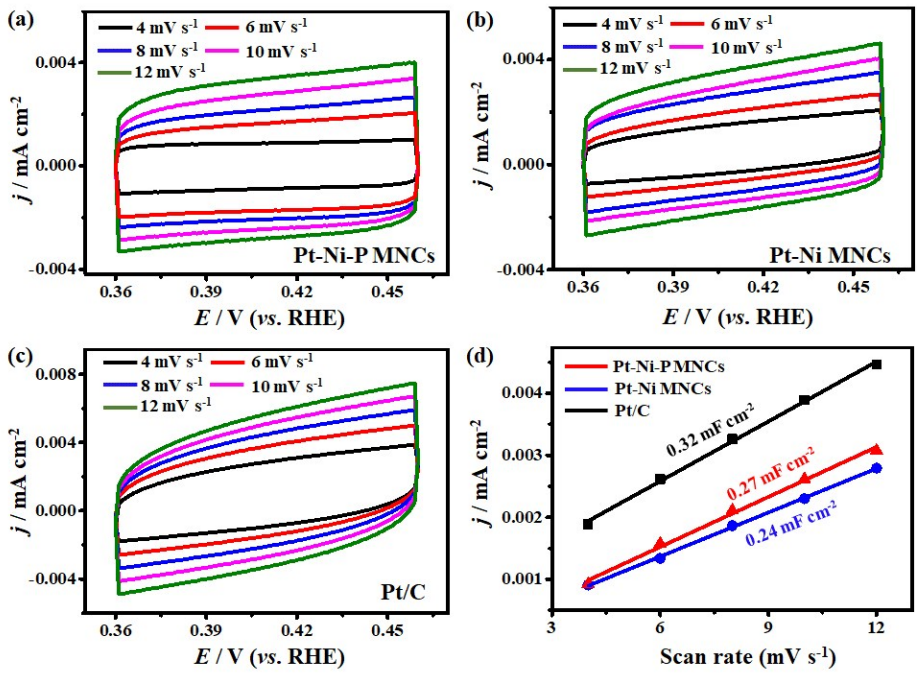

Fig. S9 Electrochemical double-layer capacitance measurements of various catalyst-modified electrodes: (a) Pt-Ni-P MNCs; (b) Pt-Ni MNCs; and (c) Pt/C. (d) Current density at 0.40 V as a function of the scan rate for the different electrodes.

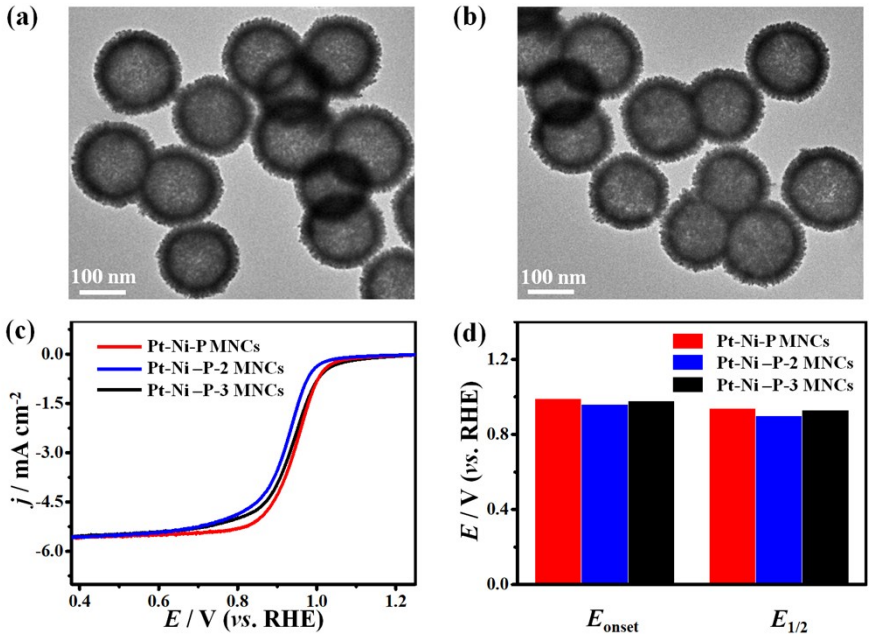

Fig. S10 TEM images of (a) Pt-Ni-P-2 MNCs (65.59 at% Pt, 5.26 at% Ni, and 29.35 at% P) and (b) Pt-Ni-P-3 MNCs (58.21 at% Pt, 17.28 at% Ni, and 24.51 at% P). (c) ORR polarization curves of the catalysts. (d) E_{onset} and $E_{1/2}$ of the catalysts.

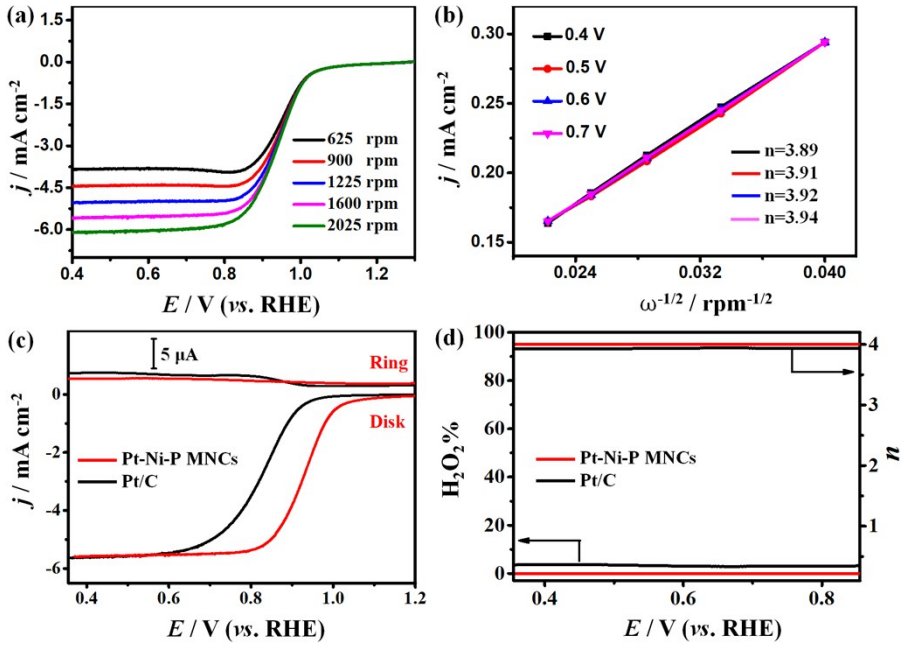

Fig. S11 (a) Rotation-rate-dependent current-potential curves of the Pt-Ni-P MNCs. (b) The electron transfer number at different potentials. (c) RRDE test in an O_2-saturated 0.1 M $HClO_4$ solution at a rotation rate of 1600 rpm. (d) Peroxide percentage and electron transfer number measured by using an RRDE test.

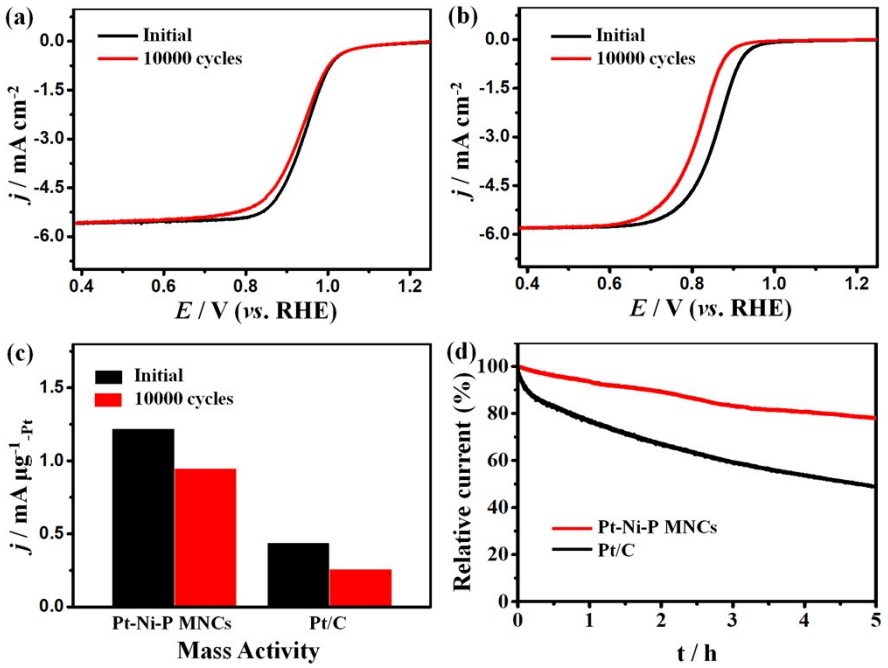

Fig. S12 ORR polarization curves of (a) Pt-Ni-P MNCs and (b) Pt/C before and after an accelerated durability test. (c) Comparisons of mass activities before and after an accelerated durability test. (d) i-t response in an O_2-saturated 0.1 M $HClO_4$ solution at a rotation rate of 1600 rpm.

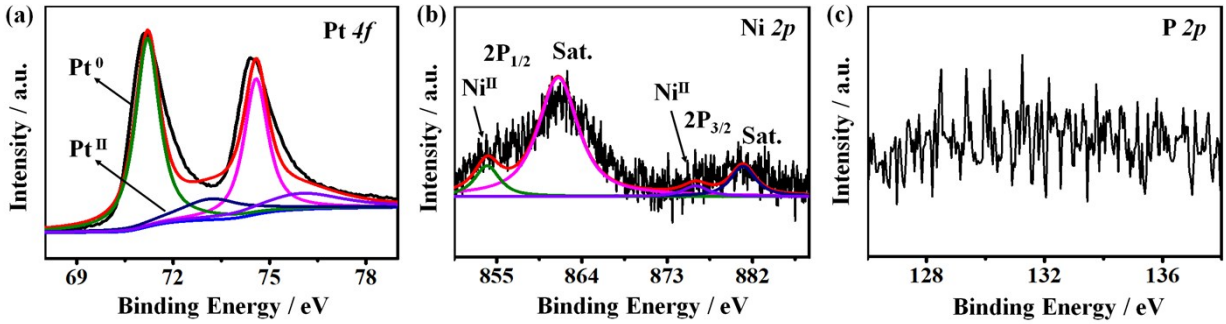

Fig. S13 XPS spectra of the Pt 4f (a), Ni 2p (b) and P 2p (c) for the Pt-Ni-P MNCs after ORR duribility test.

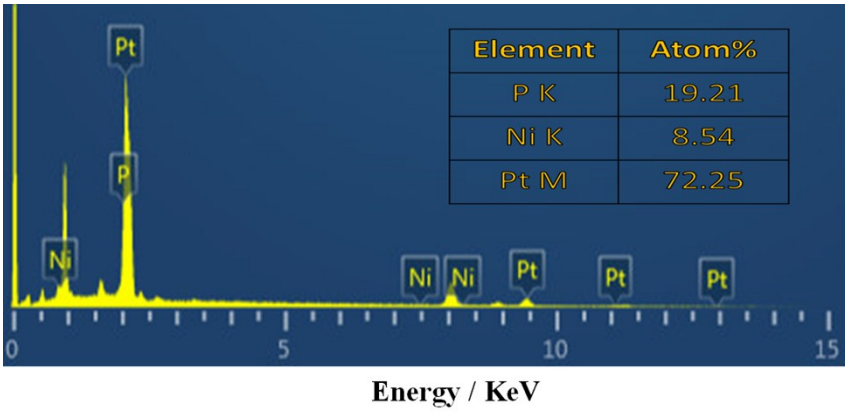

Fig. S14 EDX spectrum of the Pt-Ni-P MNCs after ORR duribility test.

Table S1. The mass activity comparison of MOR on various Pt-based electrocatalysts.

Catalyst	Condition	Scan rate ($mV\ s^{-1}$)	Mass activity (j / mA $\mu\ g^{-1}_{Pt}$)	Ref.
Pt-Ni-P MNCs	**0.5 M H_2SO_4 containing 1 M CH_3OH**	**50**	**1.22**	**This work**
Pt Nanoparticles	0.5 M H_2SO_4 containing 1 M CH_3OH	50	0.46	[1]
Dendrites PtPdCu	0.5 M H_2SO_4 containing 1 M CH_3OH	50	0.69	[2]
Hollow Pt-Pd nanodendrites	0.5 M H_2SO_4 containing 1 M CH_3OH	50	0.58	[3]
Pt Nanoparticles	0.5 M H_2SO_4 containing 1 M CH_3OH	50	0.87	[4]
Au-Pt nanodendrites	0.5 M H_2SO_4 containing 1 M CH_3OH	50	0.45	[5]
Ultrathin Pt nanowire	0.5 M H_2SO_4 containing 1 M CH_3OH	50	0.58	[6]
Au@Pd@Pt nanoparticles	0.5 M H_2SO_4 containing 1 M CH_3OH	50	0.43	[7]
Pt_1Ru_3 nanosponge	0.5 M H_2SO_4 containing 1 M CH_3OH	50	0.41	[8]

References

[1] Meng, H.; Xie, F.; Chen, J.; Sun, S.; Shen, P. K. *Nanoscale* **2011**, *3*, 5041.

[2] Chang, R.; Zheng, L.; Wang, C.; Yang, D.; Zhang, G.; Sun, S. *Appl. Catal. B: Environ.* **2017**, *211*, 205.

[3] Wang, L.; Yamauchi, Y. *J. Am. Chem. Soc.* **2013**, *135*, 16762.

[4] Yan, M.; Jiang, Q.; Zhang, T.; Wang, J.; Yang, L.; Lu, Z.; He, H.; Fu, Y.; Wang, X.; Huang, H. *J. Mater. Chem. A* **2018**, *6*, 18165.

[5] Li, Y.; Ding, W.; Li, M.; Xia, H.; Wang, D.; Tao, X. *J. Mater. Chem. A* **2015**, *3*, 368.

[6] Ruan, L.; Zhu, E.; Chen, Y.; Lin, Z.; Huang, X.; Duan, X.; Huang, Y. *Angew. Chem. Int. Ed.* **2013**, *52*, 12577.

[7] Wang, L.; Yamauchi, Y. *Chem. Mater.* **2011**, *23*, 2457.

[8] Xiao, M.; Feng, L.; Zhu, J.; Liu, C.; Xing, W. *Nanoscale* **2015**, *7*, 9467.